**Volume 45, Issue 2 | 2025**
*https://cejsr.academicjournal.io/index.php/journal/*
**ISSN: 2694-9970**

*Article*

# Impact of Etching Time on The Nanostructuring of Silicon Wafer Surfaces Using Sun Light Photochemical Method

**Hassan A. Kadhem**

1. Ministry of Education, Open Educational College, Kirkuk Center, Iraq
* Correspondence: albayaty.hassan1@yahoo.com

**Abstract:** Nanostructured porous silicon (PS) has emerged as a promising material due to its unique electronic and optical properties, which are influenced by fabrication techniques and etching parameters. Photochemical etching using sunlight as a natural energy source (S.L.PCE) offers a cost-effective, environmentally friendly alternative to industrial light sources. While prior studies explored porous silicon formation using artificial illumination, limited research has focused on the effects of etching time under concentrated sunlight. This study investigates the impact of varying etching durations (40–70 minutes) on the morphology and structural properties of PS layers formed on (111) N-type silicon wafers. Using a convex lens to focus sunlight and a fixed 40% HF concentration, etching was performed, and atomic force microscopy was employed to assess topography, thickness, and particle distribution. The results demonstrate that increased etching time leads to thinner wall structures, smaller nanoparticle diameters (101.18 nm to 66.36 nm), and thicker porous layers (9.79 nm to 51.38 nm), accompanied by an increase in surface roughness and RMS values. Statistical analysis showed negatively skewed and high-kurtosis particle size distributions, indicating non-normal distribution shapes with sharper peaks. The study is among the first to systematically evaluate the influence of solar-based etching duration on PS layer characteristics using real sunlight, avoiding artificial heating and vapor hazards. Findings offer insights for optimizing low-cost, green fabrication of nanoscale silicon for potential applications in optoelectronics, photodetectors, and sensing technologies.

**Citation:** Kadhem, H. Impact of Etching Time on The Nanostructuring of Silicon Wafer Surfaces Using Sun Light Photochemical Method. Middle European Scientific Bulletin 2024, 45(2), 95-104.

Received: 05th Mar 2025
Revised: 12th Mar 2025
Accepted: 19th Apr 2025
Published: 26th Apr 2025

**Copyright:** © 2024 by the authors. Submitted for possible open access publication under the terms and conditions of the Creative Commons Attribution (CC BY) license (https://creativecommons.org/licenses/by/4.0/)

**Keywords:** pours silicon, (PS) morphology studies, photochemical Etching, sun light photochemical etching, S,L.PCE

## 1. Introduction

A silicon nanocrystal , a small piece of Si, contains a few tens to a little ten thousands of atoms with archetypal dimensions of one to ten nanometers[1]. Regions of silicon in nano meter size surrounded by emptiness space forming as a network [2]. Porous silicon is combination between silicon and void space of nanoporous that create a micro structure and provide a large surface to volume ratio[3]. The discovery of the importance of silicon in the zero dimension was in the 1990[4]. With Canham's discovery of the phenomenon of photo luminescent (PL) in porous silicon, which was explained on the basis of the phenomenon of quantum confinement of charge carriers. "quantum confinement" means considering the approximation of electrons and holes effective mass in semiconductors and the "particle in a box" problem [5]. Solving the non-timedependent Schroedinger equation gives us the energy levels separation with inversely proportional between the energies and the square of the potential well width, (when the potential well width is small or particles in nanosize means higher energy levels). Like this approximation, means negative effective mass for the holes, which leads to an increase in the energy band gap[6].

Photoluminescence in the visible area (400-800 nm or 1.5-3 eV), which occurs after exciting the samples with a blue light source (High energy) is often considered evidence of quantum confinement. Because photoluminescence in bulk silicon is in the infrared region (1.1 eV). Quantum confinement not only expands the energy gap and thus allows for luminescence in the visible region in Si, but also enhances the efficiency of this luminescence. The bandgap in Bulk silicon is indirect, that means in order to moderate the electron - hole recombination , a phonon is needed so as to conserve crystal momentum. at room temperature ,this is an inefficient process (<0.001%). Confining carriers in real space, causing to spread their wave functions out in k-space and the band gap is became more direct-like [7]. Electronic and optical properties desirable for various applications in optoelectronics [8]energy storage [ 9 ] biomedicine [10]Photonic crystal[11], Gas sensor[12] solar cells[13] photodetector [14,15,2].

Silicon nanocrystals can be fabricated by various methods such as Photoelectrochemical etching [16,17] Laser- induced etching [18,19] Pulsed laser deposition (PLD)[20] Femtosecond-laser pulses technique [21] laser-assisted electrochemical etching [22] photochemical etching using a halogen lamp [23] electro-chemical etching [3] [4] [13] [24 [25] Aerosol techniques [1] green synthesis[26] ordinary light-assisted etching (OLAE)[27] laser-assisted etching (LAE) [14][15] [27] Stain etching [28]

The most acceptable dissolution mechanics was presented by Lehmann and Gösele, It is based on a surface bound oxidization scheme, with hole capture, and subsequent electron injection, which leads to the divalent Si oxidization state. The injected holes attack the bond between silicon and hydrogen, breaking it and being replaced by fluorine ions. The second attack of fluoride ions leads to the of evaporation hydrogen, which results in electron injection to the substrate. The back bonds between silicon and silicon are broken due to HF attack. The remaining surface silicon atoms will combine with hydrogen atoms, resulting in a silicon tetrafluoride molecule, which reacts with two molecules of HF forming $H_2SiF_4$ which later ionizes to $SiF6^{-2}$ and $2H^+$ [29].

The etching processing of Silicon in HF produce surfaces with different properties because of the various rates for etching processing that improve on the tips and on the pores walls. At the tips, because of the highest curvature radius ,the carriers are preferentially collected which is responsible for a large electric field. For densities more than a critical carrier density, The holes that reach the tips cannot be consumed all for a long time, the process of dissolution begins also on the walls of the pores, the electropolishing process takes place , this process is different for n-type silicon than for P-type silicon. Figure (1). In n-type silicon, the substrate illumination leads to the photogeneration of holes that move towards the surface, where they spread at the pits of the pores and enter the solution. The spread of these holes is responsible for limiting the formation of macropores. While permanent availability for holes in p-type silicon, it is sufficient to generate current during the etching process to form macro pores. very different structures were produce from these two different mechanisms. In n-type silicon, the carrier concentration within the porous regions can be precisely regulated through the intensity of incident light. This control allows the formation of pores with high aspect ratios, as lateral expansion is effectively suppressed. On the other hand, in p-type silicon substrates, although the lateral growth of pores can be minimized, it cannot be completely eliminated. The spatial distribution of macropores also varies depending on the surface treatment. When no pre-patterning is applied, macropores tend to appear in a random arrangement across the surface. However, when the silicon surface is patterned with etch-pits using photolithography followed by potassium hydroxide (KOH) etching, the macropores form in a well-ordered, regular pattern[30] (Figure 1).

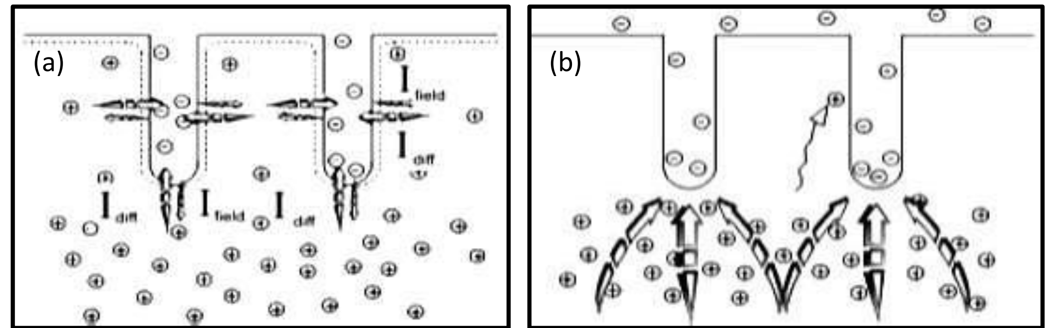


Figure (1): (a) showed how the dissolution process in p-type silicon causes expansion of pores during etching due to lateral currents during the etching process. (b) schematic diagram of the dissolution in n-type silicon, in which completely depletion of carriers in semiconductor between the pores [30].

The use of sunlight as a substitute for industrial sources (S.L.PEC) method was applied practically for the first time in 2018 where lenses of different diameters used to obtain different light intensities sufficient and appropriate to form layers of porous silicon with nanoscale dimensions that were studied using atomic force microscopy, as well as studying the electrical properties of diodes resulting from the formation of a P-N junction between the Bulk layer and porous layer obtained from photochemical etching processing. The results of the study of the electrical properties (I-V) showed different rectification properties depending on the preparation conditions [31] .

There are several factors that affect the shapes and sizes of particles that formed in the porous layer and the thickness of this layer , the proportion among these variables will produce layers with different properties these factors and variables have been presented in many research and studies : type of crystalline silicon, light power density[31], silicon resistivity etching time[23] HF acid concentration[26,32]

**2. The Practical Part**

N-type crystalline silicon with resistivity of (1-10Ω.cm ) and (111) orientation were cut in dimensions (0.5cmx0.5cm) , after cutting, they were cleaned using distilled water and ethanol. In order to remove the oxide layer formed on the surfaces of the samples, they are immersed for 10 minutes in 40% HF acid .

The system used in this study consists of a Teflon container with a diameter 7 cm , internal height 3 cm, external height 4 cm Fig.3 (a), designed in its inner center a U-shaped stand of the same material Fig.3 (c), In order the silicone samples to settle on them, which were cut to dimensions suitable with the dimensions of the backing, the Teflon container is filled with hydrofluoric acid so that it covers the upper surface of the sample by several millimeters and is placed under the sunlight collected by the lens. We used a lens with a diameter of (9 cm) and a focal length of (30 cm), the angle of inclination was adjusted Mounted on a stand that allows free movement of the lens so that the focus of the sunlight spot is ensured on the shiny side of the surface of the (mirror-like) silicon samples Fig.3 (b , c). It is possible to calculate the light power density on the surface of the lens, as the average value of the radiation intensity reaches on each square meter on earth (Solar Flux Density Reaching Earth) is about 1367 $w/m^2$[33,34]. In this study, two methods were used to calculate the light power density incident on the samples surface: first by using a Digital Light Meter (Lutron LX-103), second using the arithmetic method, assuming that the realistic average irradiance value of 1000 $W/m^2$ (equivalent to 100 $mW/cm^2$) was adopted as the standard working condition. The total incident power was estimated by multiplying the lens area by the solar irradiance per square centimeter, resulting in a value of 6360 mW. When this amount of light energy is concentrated onto a 1 $cm^2$ sample surface, the resulting power density is 6360 $mW/cm^2$, or 6.36 $W/cm^2$. If the same light is instead focused onto a 0.25 $cm^2$ area, the intensity increases by a factor of four, reaching 25.44 $W/cm^2$. This level of energy is sufficient to drive the etching process. The experimental setup in this work achieved this same energy level, as presented in Table 1.

Table (1) Shows the lens parameters and the calculation of the luminous intensity on the surface of the samples

| *Lens radius (r) (cm)* | *lens area (cm²) A=π r²* | *Optical power over the entire surface of the lens P(mw)* | *light intensity focused on the sample area 1 cm² I(mw/cm²)* | *light intensity focused on the sample area 0.25 cm²* |
|---|---|---|---|---|
| 4.5 | 63.6 | $100\frac{mw}{cm^2}$ x 63.6 $cm^2$ =6360 mw | $6360\frac{mw}{cm^2}$ Or (63.6) $\frac{W}{cm^2}$ | $\frac{6.36\frac{W}{cm^2}}{0.25cm^2}$ =25.44 w |

Figure 2 illustrates the experimental setup for Sunlight Photochemical Etching (S.L.PCE) of silicon wafers. It includes (a) the chemical reagents and lens system, (b) the illuminated Teflon container under focused sunlight, and (c) a schematic showing the lens, sample holder, and HF acid arrangement for nanoscale surface etching [19].

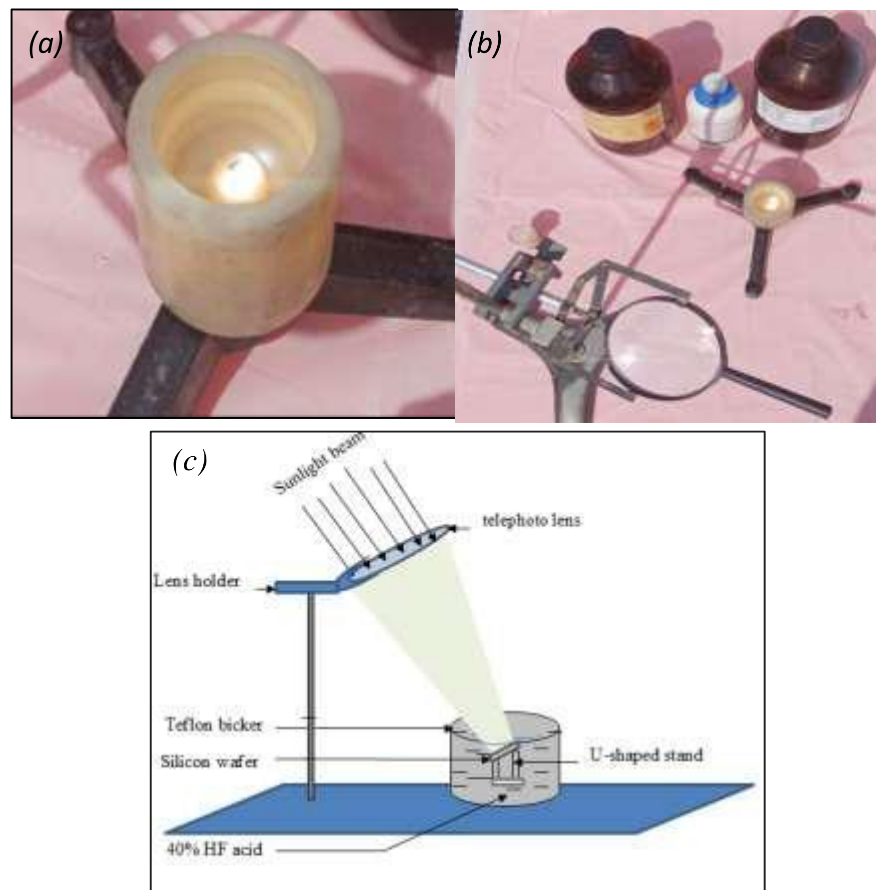


Figure (2): (a) The Teflon container (b) showing the setup of the Sun light photochemical etching (S.L.PCE) system (c) a schematic diagram of the experimental set-up.

It is considered high energy and is available at lower costs compared to other light sources that are accompanied by some physical and health damages, the associated heat when using industrial sources such as halogen and tungsten leads to rapid evaporation of the acid used, which requires compensating for the shortage of acid continuously, in addition to the health damages resulting from inhalation of acid vapor [20]. While these cases do not occur in this method that has been adopted (photochemical etching using

sunlight ). The appearance of some bubbles on the surface of the sample during the experiment is evidence of the beginning of the chemical dissolution process, which are hydrogen bubbles resulting from the chemical dissolution reactions of silicon[31].After a short period, the surface color also changed to a buffish brown color (the color of iron rust) another evidence of the formation of the porous layer, This process continues along the etching time, which is fixed for all samples (60min). after completing the Preparation process , the samples are removed from the Teflon container and placed in plastic containers filled with methanol in order to preserve them from oxidation .

**3. Results and Discussion**

Atomic force microscopy results showed the formation of nano sized porous silicon layers whose thickness increased from 9.79 nm to 51.38 nm Figure( 3) and their surface roughness increased from 2.28 nm to 9.13 nm the Root Mean Square (RMS) roughness changed from 2.5nm to 11nm with increasing photochemical etching time from 40 min. to 70 min respectively .

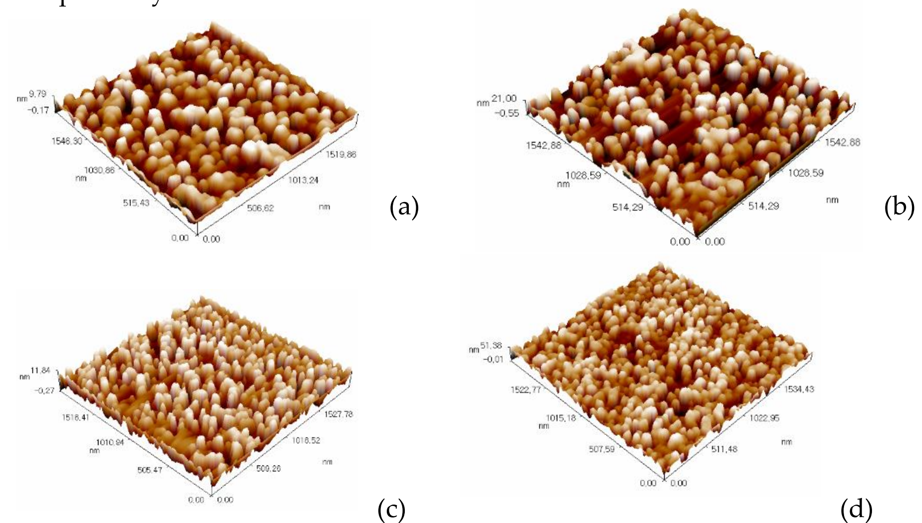


Figure ( 3): AFM image of the porous layer in silicon prepared at different etching time of (a) 40, (b) 50, (c) 60, and (d) 70 min.

These changes in the (RMS), roughness and thickness of the porous layer can be explained by the mechanism through which the holes contribute to the etching process. In N-type silicon, the holes are photo generated, depending on the light intensity falling on the surface as well as the doping density of the substrate . These holes move inside the sample towards the surface to compensate for those that were consumed in the dissolution processes (hole injection and attack on a Silicon –Hydrogen bond by a fluoride ion). In any case, the current density of the holes must be less than the critical factor to avoid the occurrence of the electroplating process[35]. The holes that reach the pore bottom curve contribute more to vertical dissolution, figure (1- b )[30], as the etching time for this process increases, the thickness and roughness of the porous layer increases, Table (2) and Figure (4).

Table (2): Shows information about porous silicon layers

| Sample Etching time Min | root mean square (nm) | Layer thickness (nm) | Average of surface roughness (nm) | Avg. Diameter (nm) |
|---|---|---|---|---|
| 40 | 2.65 | 9.79 | 2.28 | 101.18 |
| 50 | 6.22 | 21 | 5.39 | 72.00 |
| 60 | 3.13 | 11.84 | 2.66 | 68.94 |
| 70 | 11 | 51.38 | 9.13 | 66.36 |

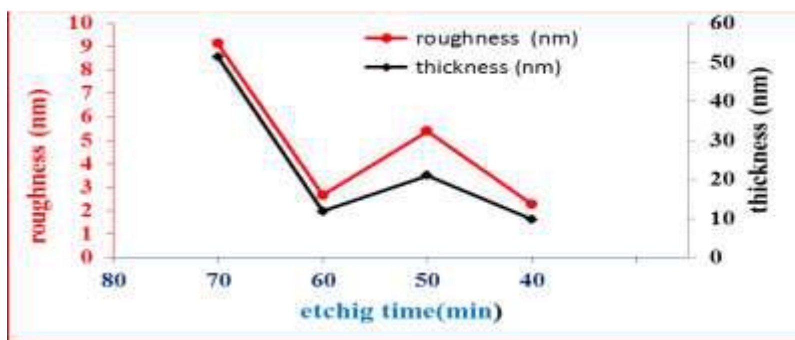


Figure (4). The thickness and roughness of the samples at each etching time

While the holes that reach the top of the sample surface contribute more to horizontal dissolution (Side etching), which leads to a reduction in the thickness of the walls between the pores and their partial erosion, forming particles with different diameters, sizes and shapes within the nanoscale dimension . Their size decreases with increasing etching time. Thisexplains the change inthe particles diameter formed onthe surfaces from101.18 nm to 66.36 nm with a change in time. Etching from 40 minutes to 70 minutes Figure (5).

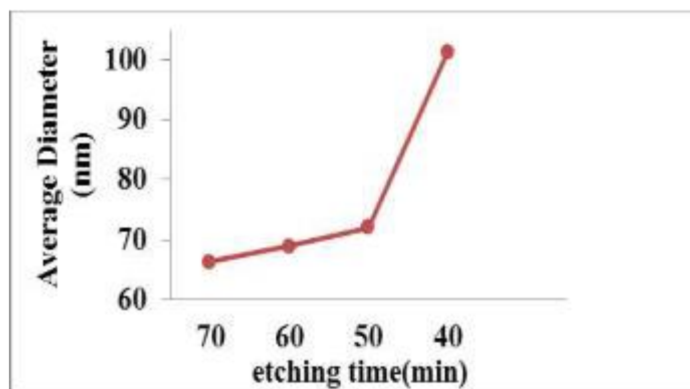


Figure (5): average diameters of nanoparticles at each etching time.

Figure (6) provides an explanation of the statistical distribution of particles formed on the surfaces of porous silicon layers , the percentage of diameters and sizes of these particles, as well as the cumulative percentage, and information about skewness and kurtosis figure (6- a, c, d) shows the statistical distributions of the particles formed on the samples prepared under an etching time of 40, 60, and 70 minutes with negative skewness values (- 0.117, - 0.185 , - 0.434) (skewness is a measure of the asymmetry of the probability distribution of a real-valued random variable about its mean)[36], for average diameter of the particles (101.18, 68.94 , 66.36) nm respectively . While the sample that was prepared at an etching time of 50 minutes, the statistical studies showed a small positive skewness value (0.000471), with a probability distribution close to the normal distribution, (a skewness value of normal distribution equal to zero) Figure (6 - b) table (3) .

Table (3): Amplitude parameters for the produced layers

| Etching time min | Skewness of surface | kurtosis of surface | average distance between a peak to peak(nm) | ten point height (nm) |
|---|---|---|---|---|
| 40 | - 0.117 | 1.89 | 9.96 | 5.39 |
| 50 | 0.000471 | 1.8 | 21.5 | 21.5 |
| 60 | -0.185 | 2 | 12.1 | 6.72 |
| 70 | - 0.434 | 2.51 | 51.4 | 51.3 |

Figure 6 presents histograms and cumulative distributions of nanoparticle diameters on porous silicon surfaces etched for 40, 50, 60, and 70 minutes. The data reveal a decreasing trend in average particle size with longer etching durations, indicating finer nanostructure formation and enhanced uniformity as etching progresses under constant photochemical conditions [30] [31].

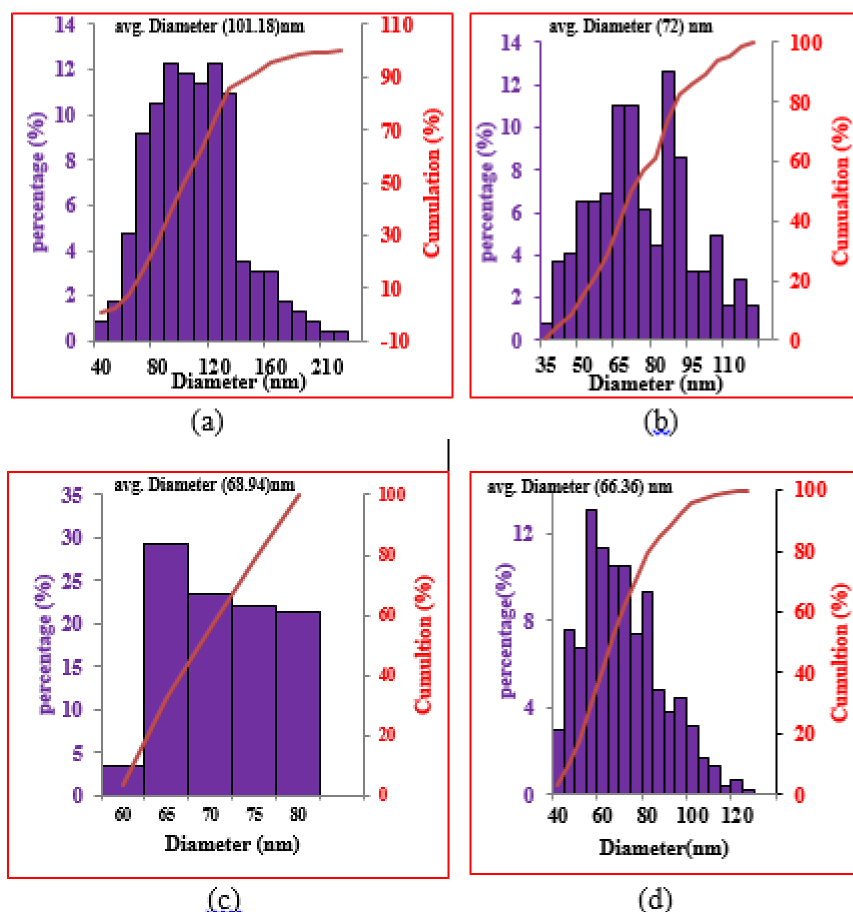


Figure (6):The statistical distribution of nanoparticle sizes on the surface of the porous silicon layer prepared at different etching time : (a) 40, (b) 50, (c) 60, and (d) 70min

Another important statistical measurement provided by the atomic force microscope regarding the distribution of nanoparticles on surfaces is kurtosis «kurtosis is a statistical number that tells us if a distribution is taller or shorter than a normal distribution . If a distribution is similar to the normal distribution, the Kurtosis value is 0. If Kurtosis is greater than 0, then it has a higher peak compared to the normal distribution. If Kurtosis is less than 0, then it is flatter than a normal distribution » [36]. Table (3) shows values of kurtosis higher than zero for all samples, which means that the statistical distributions of nanoparticles formed on the surfaces of the samples are higher than the normal distribution, (kurtosis of normal distribution is zero). Figure (7) shows the statistical measurements of both the skewness and kurtosis of the distribution of nanoparticles formed on the surfaces of porous silicon samples as a function of the etching time.

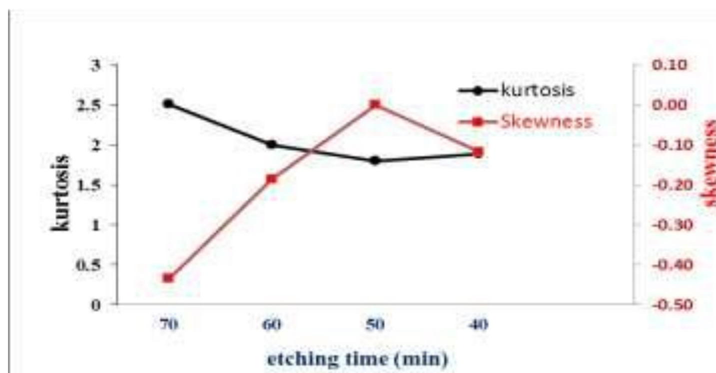


Figure (7). surface kurtosis (black line) and skewness (red line) for different etching time.

## 4. Conclusion

The shape and size of nanoparticles formed on the surfaces of samples etched by the photochemical method focusing of sunlight is a function of several parameters during the preparation process, including: HF acid concentration, density of substrate doping, etching time , type of silicone , intensity of the light and the distribution of this light density on the surface. increasing the etching time led to the creation of smaller particles, and an increase in (RMS), thickness and roughness of this layers as a result of two types of dissolution to which the photogenerated holes contribute: 1) the dissolution processes which are close to the surface towards the sides of the pores (horizontal etching) lead to reducing the thickness of the walls between the pores and partially dissolving them, thus forming particles with smaller diameters. 2) Dissolution processes towards depth, which occur at the bottom and sides of the pores, they lead to an increase in the thickness of the porous layer, Both of the above processes increase with increasing etching time. Light passing through a converging lens undergoes a Gaussian distribution, which means that the etching processes are greater at the center of the beam than at its edges. So the particles formed in the center of the sample are smaller and their diameters increase as we approach the edge of the sample due to incident light distribution Therefore, the sizes and diameters of the particles formed on the surface are close to the same distribution above.

## REFERENCES

[1] E. A. Boer, Synthesis, Passivation and Charging of Silicon Nanocrystals, Ph.D. dissertation, California Institute of Technology, Pasadena, California, 2001. [Online]. Available: https://thesis.library.caltech.edu/145/1/00EBoer_thesis_no_bib.pdf

[2] R. A. Ismail, A. M. Alwan, and A. S. Ahmed, "Preparation and characteristics study of nanoporous silicon UV photodetector," Appl. Nanoscience, vol. 7, no. 1–2, pp. 9–15, 2017. [Online]. Available: https://doi.org/10.1007/s13204-016-0544-9

[3] A. A. Ensafi, F. Rezaloo, and B. Rezaei, "Electrochemical sensor based on porous silicon/silver nanocomposite for the determination of hydrogen peroxide," Sensors and Actuators B: Chemical, vol. 231, pp. 239–244, 2016. [Online]. Available: https://doi.org/10.1016/j.snb.2016.03.018

[4] L. T. Canham, "Silicon quantum wire array fabrication by electrochemical dissolution of wafers," Appl. Phys. Lett., vol. 57, pp. 1046–1048, 1990. [Online]. Available: https://www.researchgate.net/publication/224423651

[5] G. C. John and V. A. Singh, "Porous silicon: theoretical studies," Phys. Rep., vol. 263, no. 2, pp. 93–151, 1995. [Online]. Available: https://doi.org/10.1016/0370-1573(95)00052-4

[6] A. Zunger and L.-W. Wang, "Theory of silicon nanostructures," Appl. Surf. Sci., vol. 102, no. 2, pp. 350–359, 1996. [Online]. Available: https://doi.org/10.1016/0169-4332(96)00078-5

[7] L. T. Canham, "Progress towards understanding and exploiting the luminescent properties of highly porous silicon," Optical Properties of Low Dimensional Silicon Structure, vol. 244, pp. 81–94, 1993. [Online]. Available: https://doi.org/10.1007/978-94-011-2092-0_10

[8] Y. L. Khung, "Hydrosilylation of porous silicon: Unusual possibilities and potential challenges," Adv. Colloid Interface Sci., vol. 338, 103416, 2025. [Online]. Available: https://doi.org/10.1016/j.cis.2025.103416

[9] Z. Yuan et al., "A porous silicon/graphite anode modified with Li3PO4 and polyethylene oxide (PEO) for highly Li+ dynamic and stable lithium-ion batteries," J. Energy Storage, vol. 122, 116621, 2025. [Online]. Available: https://doi.org/10.1016/j.est.2025.116621

[10] R. H. Kang et al., "Recent advances of macrostructural porous silicon for biomedical applications," ACS Appl. Mater. Interfaces, vol. 17, no. 4, pp. 5609–5626, 2025. [Online]. Available: https://doi.org/10.1021/acsami.4c18296

[11] M. J. Goodwin et al., "Deep reactive ion etching of cylindrical nanopores in silicon for photonic crystals," Nanotechnology, vol. 34, no. 22, 225301, 2023. [Online]. Available: https://doi.org/10.1088/1361-6528/acc034

[12] S. H. Salman et al., "Ammonia gas sensing using porous silicon," J. Phys.: Conf. Ser., vol. 2857, 012051, 2024. [Online]. Available: https://doi.org/10.1088/1742-6596/2857/1/012051

[13] M. J. Khalifa, "Effect of increasing etching time on the efficiency of porous silicon solar cells," J. Phys.: Conf. Ser., vol. 2432, 012019, 2023. [Online]. Available: https://doi.org/10.1088/1742-6596/2432/1/012019

[14] M. A. Abed and F. A.-H. Mutlak, "Production and characterization of porous silicon via laser-assisted etching as photodetector: Effect of different HF concentrations," J. Opt., 2023. [Online]. Available: https://doi.org/10.1007/s12596-023-01455-9

[15] N. H. Harb and F. A.-H. Mutlak, "Production and characterization of porous silicon via laser-assisted etching: Effect of gamma irradiation," Optik, vol. 246, 167800, 2021. [Online]. Available: https://doi.org/10.1016/j.ijleo.2021.167800

[16] A. A. Urabe, U. M. Nayef, and R. Kamel, "Influence study of etching time for porous silicon on morphological, optical, electrical and spectral responsivity properties," Al-Mustansiriyah J. Sci., vol. 34, no. 2, 2023. [Online]. Available: https://doi.org/10.23851/mjs.v34i2.1223

[17] T. S. Atta et al., "Porous silicon fabrication by electrochemical and photoelectrochemical methods," J. Phys.: Conf. Ser., vol. 1963, 012153, 2021. [Online]. Available: https://doi.org/10.1088/1742-6596/1963/1/012153

[18] H. S. Mavi et al., "Spectroscopic investigations of porous silicon prepared by laser-induced etching of silicon," J. Phys. D: Appl. Phys., vol. 34, no. 3, p. 292, 2011. [Online]. Available: https://doi.org/10.1088/0022-3727/34/3/307

[19] Z. Hassan and K. Omar, "Laser-induced etching parameters impact on optical properties of the silicon nanostructures," Sci. China Technol. Sci., vol. 54, no. 1, pp. 58–62, 2011. [Online]. Available: https://doi.org/10.1007/s11431-010-4179-x

[20] M. A. Fakhri et al., "Effect of laser flounce on the optoelectronic properties of nanostructured GaN/porous silicon prepared by pulsed laser deposition," Sci. Rep., vol. 13, 14746, 2023. [Online]. Available: https://doi.org/10.1038/s41598-023-41396-8

[21] J. Long et al., "Formation of dense nanostructures on femtosecond laser-processed silicon carbide surfaces," Surfaces and Interfaces, vol. 28, 101624, 2022. [Online]. Available: https://doi.org/10.1016/j.surfin.2021.101624

[22] A. A. Jabbar et al., "WO3 nanoparticles-embedded porous silicon: Dual-function materials synthesized via laser ablation and electrochemical etching for advanced photodetection and gas sensing applications," Optical Materials, vol. 163, 116971, 2025. [Online]. Available: https://doi.org/10.1016/j.optmat.2025.116971

[23] A. M. E. Ibrahim, H. A. Kadhem, and A. H. Jasem, "Study the effect resistivity slide and the time of etching on silicon surfaces morphology of producing photovoltaic method," Tikrit J. Pure Sci., vol. 21, no. 7, pp. 152–161, 2016. [Online]. Available: https://doi.org/10.25130/tjps.v21i7.1122

[24] D. H. Jwied, U. M. Nayef, and F. A. H. Mutlak, "Synthesis of porous silicon by electrochemical etching for gas sensor application," Eng. Technol. J., vol. 40, no. 4, pp. 555–562, 2022. [Online]. Available: https://doi.org/10.30684/etj.v40i4.2064

[25] S. Naidu et al., "Silicon nanoparticles: Synthesis, uptake and their role in mitigation of biotic stress," Ecotoxicol. Environ. Saf., vol. 255, 114783, 2023. [Online]. Available: https://doi.org/10.1016/j.ecoenv.2023.114783

[26] N. M. Kadum, "Study the Properties of Porous Silicon for P-type and N-type Bulk Silicon," Univ. of Kerbala, College of Education for Pure Sciences, 2021. [Online]. Available: https://uokerbala.edu.iq/wp-content/uploads/2021/09/Rp-Study-the-Properties-of-Porous-Silicon-for-P-type-and-N-type-Bulk-Silicon.pdf

[27] A. A. Thahe et al., "Engineered etching and laser treatment of porous silicon for enhanced sensitivity and speed of Pt/n-PSi/Pt UV photodetectors," Nanoscale Adv., 2025. [Online]. Available: https://doi.org/10.1039/D5NA00137D

[28] S. Juyal et al., "Porous silicon formation by stain etching with FeCl3 oxidant," AIP Conf. Proc., vol. 2481, 020027, 2022. [Online]. Available: https://doi.org/10.1063/5.0104526

[29] V. Lehmann and U. Gosele, "Porous silicon formation: A quantum wire," Appl. Phys. Lett., vol. 58, pp. 856–858, 1991. [Online]. Available: https://doi.org/10.1063/1.104512

[30] V. Lehmann and U. Grunin, "Thin Solid Films," vol. 297, p. 13, 1997.

[31] I. K. Jassim, A. Y. Khudair, and H. A. Kadhem, "Preparation of porous silicon wafers using sunlight photochemical etching (SLPCE)," Tikrit J. Pure Sci., vol. 23, no. 7, 2018. [Online]. Available: https://doi.org/10.25130/tjps.v23i7.700

[32] H. A. Kadhem et al., "Study the effect of hydrofluoric (HF) concentration on the topography of the porous silicon layer prepared by sunlight photochemical etching (SLPE)," East Eur. J. Phys., vol. 3, pp. 340–345, 2023. [Online]. Available: https://doi.org/10.26565/2312-4334-2023-3-35

[33] G. Kopp and J. L. Lean, "A new, lower value of total solar irradiance: Evidence and climate significance," Geophys. Res. Lett., vol. 38, L01706, 2011. [Online]. Available: https://doi.org/10.1029/2010GL045777

[34] H. Li et al., "Solar constant values for estimating solar radiation," Energy, vol. 36, no. 3, pp. 1785–1789, 2011. [Online]. Available: https://doi.org/10.1016/j.energy.2010.12.050

[35] O. Bisia, S. Ossicini, and L. Pavesi, "Porous silicon: A quantum sponge structure for silicon-based optoelectronics," Surf. Sci. Rep., vol. 38, pp. 1–126, 2000. [Online]. Available: https://www.academia.edu/32023100

[36] R. Shanmugam and R. Chattamvelli, "Skewness and Kurtosis," in Statistics for Scientists and Engineers, pp. 89–110, 2016. [Online]. Available: https://doi.org/10.1002/9781119047063.ch4